PHYSICAL REVIEW B VOLUME 53, NUMBER 21 1 JUNE 1996-I

# Thermopower of single-crystal $\mathrm{Nd}_{1-x}(\mathrm{Sr,Pb})_x\mathrm{MnO}_{3-\delta}$

Vincent H. Crespi, Li Lu, Y. X. Jia, K. Khazeni, A. Zettl, and Marvin L. Cohen
*Department of Physics, University of California at Berkeley, Berkeley, California 94720*
*and Materials Sciences Division, Lawrence Berkeley Laboratory, Berkeley, California 94720*

(Received 21 December 1995)

We report measurements of the thermopower of the single-crystal manganite perovskite $\mathrm{Nd}_{1-x}(\mathrm{Sr,Pb})_x\mathrm{MnO}_{3-\delta}$ from 4.2 to 350 K at zero and finite magnetic field. The sign and magnitude of the thermopower above the magnetic transition are doping dependent. The magnitude of the thermopower drops sharply below the transition to the magnetically ordered state. At lower temperatures the thermopower changes sign from negative to positive with decreasing temperature in the range 100–150 K. Implications for the temperature-dependent electronic structure and scattering processes in this temperature range are discussed. The high-temperature behavior is interpreted within a lattice polaron model. Further analysis suggests a form of variable-range hopping conduction at high temperatures. [S0163-1829(96)03121-9]

Manganites of the general form $R_{1-x}A_x\mathrm{MnO}_3$ ($R$=rare earth or related species, $A$=alkaline earth or lead) at doping levels $x \approx 0.2-0.6$ often exhibit a large magnetoresistance associated with a metal-insulator transition at temperature $T_{\mathrm{MI}}$ which can vary from ~30 to above 300 K. While the resistivity, magnetization, and magnetoresistivity of these materials have been studied extensively,[1–16] the temperature-dependent thermoelectric power near the magnetic transition has not yet been reported. We report measurements of the thermopower $S(T)$ at zero and applied magnetic field from 4.2 to 350 K in the manganites $\mathrm{Nd}_{1-x}(\mathrm{Sr,Pb})_x\mathrm{MnO}_{3-\delta}$ at two distinct doping levels. The thermopower $S(T)$ provides a useful probe of the transport processes in these interesting and potentially technologically useful materials. In the low-temperature metallic phase the thermopower is related to changes in electronic structure and scattering processes with variations in temperature, doping and magnetization. In the insulating phase the temperature-dependent thermopower can provide information on the energy dependence of the parameters governing the high-temperature charge transport.

Single-crystal $\mathrm{Nd}_{1-x}(\mathrm{Sr,Pb})_x\mathrm{MnO}_{3-\delta}$ samples were synthesized following the techniques of (Refs. 12 and 17). Samples from the synthesis batches used in this study were characterized by x-ray diffraction, scanning electron microscopy, energy dispersive x-ray spectroscopy (EDX), magnetization, and resistivity measurements.[13] Magnetization measurements confirmed the close association between the transition to the low-temperature ferromagnetic phase and the abrupt drop on the resistivity. X-ray diffraction along the (100) axis of one crystal revealed narrow cubic diffraction peaks with an extremely low background. EDX measurements on several locations of sample 1 yielded a uniform stochiometry of $\mathrm{Nd}_{0.57}\mathrm{Pb}_{0.39}\mathrm{MnO}_{3-\delta}$. EDX measurements on a crystal from the same synthesis batch as samples 2 and 3 yielded a uniform stochiometry of $\mathrm{Nd}_{0.5}(\mathrm{Sr}_{0.36}\mathrm{Pb}_{0.14})\mathrm{MnO}_{3-\delta}$.[14] A higher 2+ cation doping level of samples 2 and 3 relative to sample 1 is consistent with the substantially lower resistivities of samples 2 and 3, as will be discussed later.

For the present study a heat current was applied through the long axis of the parallelopiped crystals of typical dimensions 0.1×0.3×1.0 mm. Thermocouple leads and voltage leads were attached on opposite sides of the largest crystal faces. During temperature sweeps the sample temperature was controlled to within ±20 mK of target temperatures and $\Delta T$ was varied between 0 and roughly 0.5 K at a rate of 0.001 Hz.

Figures 1, 2, and 3 show the temperature-dependent thermopower and resistivity for three samples at 0 and 5 (or 6) T. The samples are numbered in order of decreasing resistivity

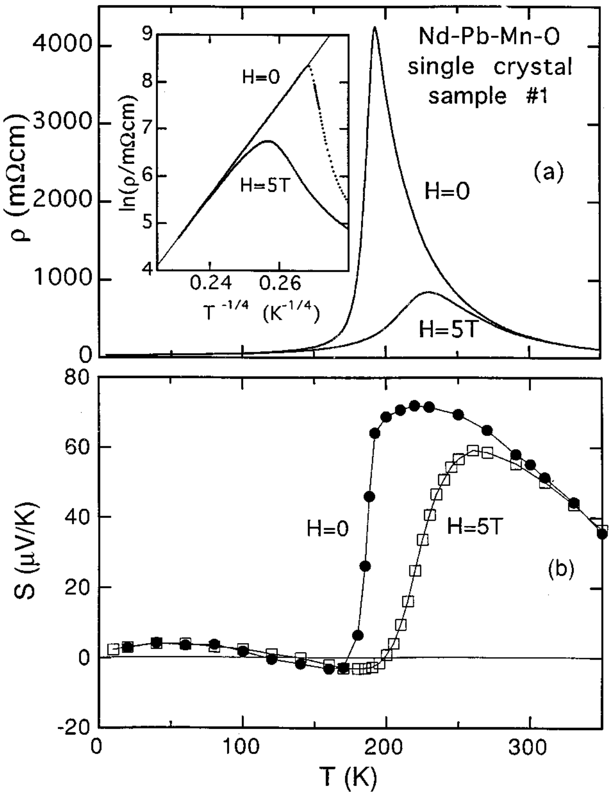

FIG. 1. Temperature dependence of the resistivity and thermopower of sample 1 at zero field and 5 T. The inset shows the linearity of the logarithm resistivity versus inverse temperature to the one-fourth.

0163-1829/96/53(21)/14303(6)/$10.00

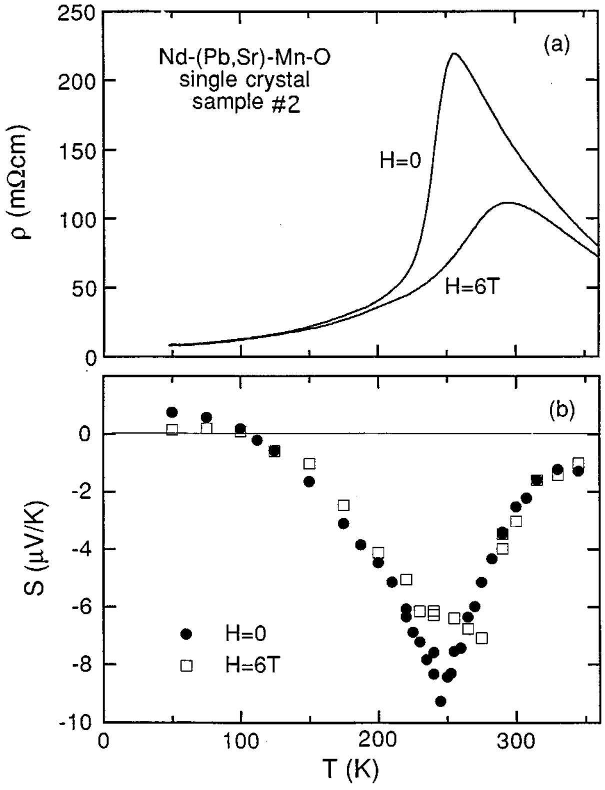

FIG. 2. Temperature dependence of the resistivity and thermopower of sample 2 at zero field and 6 T.

at 300 K, a temperature comfortably above the resistive transition. Since resistivity decreases with increasing 2+ cation concentration, this sequence is also the order of increasing hole doping.[18] The lower resistive transition temperature $T_{\mathrm{MI}}$ of sample 1 is consistent with a substantially lower doping level.[11,16] We note that the difference in resistivity between samples 2 and 3 is slight, so that the relative doping levels of these two samples is less certain.

Figure 4 shows the field-dependent thermopower for sample 3 at three different temperatures around the transition. Below (above) the transition, the thermopower increases (decreases) with increasing field, consistent with a shift of the thermopower peak to higher temperatures. The field dependence of the resistivity shown in the upper portion of Fig. 4 is similar to that seen previously in many polycrystalline samples.

Certain reproducible features can be discerned in the data for the temperature-dependent thermopower. The low-temperature thermoelectric power is positive for all materials, changing sign around 100–150 K. Near the resistive transition temperature $T_{\mathrm{MI}}$ the thermopower collapses from large values ($\sim 10-100$ $\mu V/K$) at higher temperatures to lower values ($\sim 1$ $\mu V/K$) more characteristic of metallic conduction. Application of a magnetic-field shifts, depresses and broadens the thermopower of all samples in a manner reminiscent of the changes in resistivity under the same field.

Other features appear to be doping dependent. For samples 2 and 3 the peak thermopower is negative with magnitude $\sim 9$ $\mu$V/K. For the lower-doped sample 1 the peak thermopower is positive with magnitude $\sim 70$ $\mu$V/K. These results suggest that the doping level determines the sign and magnitude of the peak thermopower.

Finally, the temperature dependence of the thermopower above the transition is sample dependent even for small differences in doping. Samples 2 and 3, with very similar forms for $S(T)$ below $T_{\mathrm{MI}}$, have different temperature dependent high temperatures. Sample 2 has a sharp peak in $S$ near $T_{\mathrm{MI}}$, whereas the thermopower for sample 3 is roughly temperature independent above the magnetic transition.

We first analyze the nearly sample-independent low-temperature thermopower. The uniform behavior at low temperatures is interesting in light of the pronounced differences between samples in the thermopower near and above $T_{\mathrm{MI}}$. If the transport is dominated by carriers in the vicinity of the Fermi energy and we neglect spin-dependent contributions, then the thermopower can be written in terms of the energy derivative of the conductivity,

$$S=\frac{\pi^2}{3}\frac{k^2T}{e}\left[\frac{\partial \ln\sigma(E)}{\partial E}\right]_{E=E_F} \qquad (1)$$

with $k$ Boltzmann's constant and $e$ the charge of an electron ($e<0$). For cubic metallic systems $\sigma(E)$ is determined by the integral over isoenergetic surfaces of the product of the scattering time and the Fermi velocity.

In the low-temperature spin-ordered state a local-spin-density approximation calculation yields a nearly half-metallic band structure, with a high density of states in the partially filled Mn-derived lower energy majority-spin bands and a low density of states in the narrower minority-spin bands.[19] The relatively large bandwidth of the dominant spin-majority bands suggests a weak energy dependence to the conductivity, a result consistent with the small absolute magnitude of thermopower at low temperatures. Below 100–150 K the thermopower for both samples is positive, implying that the product of Fermi velocity and scattering time tends to decrease with increasing energy. We tentatively conclude that conduction for $S>0$ at low temperatures is primarily holelike. The sign change near 100–150 K motivates a more detailed discussion of the band structure. Treating the doping as an ordered supercell of 2+ and 3+ ions, the positions of the different Mn-derived conduction bands depends on the local concentration of 2+ and 3+ ions, with bands primarily deriving from Mn atoms near 3+ ions having lower energy than bands deriving from Mn atoms near 2+ atoms. Qualitatively, for a cation superlattice, one obtains a ''ladder'' of energy bands offset in energy relative to each other, each filled with carriers to differing degrees.[19] The positions of the band minima in this ladder apportion between the $\Gamma$ point and the edge of the zone depending on the periodicity of the supercell. Cation disorder can then be thought of as introducing an impurity scattering potential which randomly displaces the dopants from their supercell positions and broadens the bands. The energy dependence of interband scattering for such a ladder of offset bands yields a nonmonotonic energy dependence for the conductivity, making it plausible for temperature-dependent anisotropy in the scattering time and thermal broadening of the Fermi surface to induce sign changes in the thermopower. The similarity in the temperature of the sign change for samples at different doping levels is surprising.[20] The sensitivity of the low-temperature thermopower to the band structure and interband

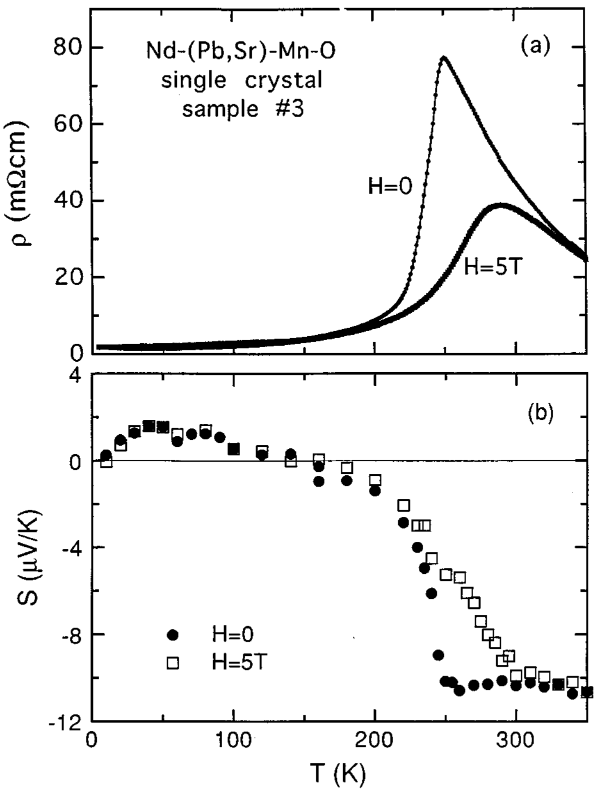

FIG. 3. Temperature dependence of the resistivity and thermopower of sample 3 at zero field and 5 T.

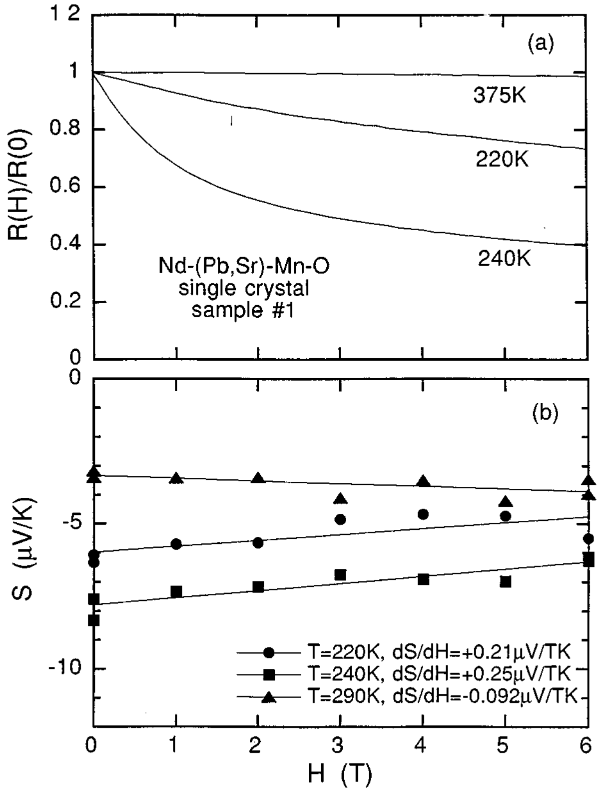

FIG. 4. Magnetic-field dependence of the resistivity and thermopower for sample 3.

scattering may provide a stringent test for detailed electronic-structure calculations.

As the temperature approaches $T_{\mathrm{MI}}$ from below the Mn-derived spin-majority and spin-minority bands fuse into a single disorder-broadened partially filled manifold of electronic states. The pronounced temperature dependence of the electronic structure is consistent with the strong temperature dependence of $S$ just below $T_{\mathrm{MI}}$. Further discussion of the high-temperature thermopower is predicated upon knowledge of the high-temperature conduction process.

Insight into the high-temperature conduction can perhaps be gained by noting that the related lightly doped manganite $\mathrm{La}_{0.83}\mathrm{Sr}_{0.17}\mathrm{MnO}_3$ undergoes a magnetically driven transition between orthorhombic and rhombohedral structures.[21] Since the double-exchange model[22–24] implies that magnetic transitions in this material are closely associated with changes in electronic structure, this exceptional magnetostructural coupling suggests a strong coupling between electronic and lattice degrees of freedom. At higher doping levels, when screening is more important, the coupling matrix elements may not be sufficient to induce a structural phase transition but may be large enough to induce local lattice distortions and consequent polaron formation in the spin-disordered high-temperature phase. Alternatively, cation disorder may be sufficient to induce Anderson localization in the spin-disordered phase, an idea proposed by Pickett and Singh.[19] For concreteness, we concentrate upon the polaron model and later discuss the relationship to other mechanisms for charge localization.

Within a double-exchange lattice polaron picture, the presence of spin disorder above $T_{\mathrm{MI}}$ reduces the Fermi velocity sufficiently that the lattice distorts around conduction electrons and produces small polarons.[13,14,25] Equation 1 for the thermopower is valid whether the transport is via metallic conduction or hopping.[28] If the conduction in the high-temperature phase proceeds via hopping of polarons with $\sigma\sim\sigma_0 e^{-E_a/T}$,[29] we obtain for the thermopower

$$S=\frac{\pi^2}{3}\frac{k}{e}\left[kT\frac{d(\ln\sigma_0)}{dE}-\frac{dE_a}{dE}\right]_{E=E_F}\tag{2}$$

with $E_a$ the hopping barrier. Spin disorder and cation disorder induce a random distribution of hopping barriers about the characteristic value, an effect which we neglect for the moment. The Einstein relation implies that the prefactor $\sigma_0$ is proportional to the density of states at the Fermi level.[28] Two terms then contribute to the thermopower: the energy dependence of the density of states and the energy dependence of the hopping barrier.[30]

To proceed further we require knowledge of the energy dependence of the electronic structure. Qualitatively, doping with 2+ cations gradually empties the Mn-derived bands at the Fermi level. From a supercell-plus-disorder point of view, at a given doping level above half emptying ($x$ less than roughly 0.5) many different bands in the ''ladder'' are each partially filled, yielding a multisheeted Fermi surface with an average Fermi velocity which increases with increasing 2+ cation concentration. Although the transition temperature as a function of doping for $\mathrm{Nd}_{1-x}(\mathrm{Sr,Pb})_x\mathrm{MnO}_{3-\delta}$ has not yet been mapped out, it is expected to be similar to that of $\mathrm{La}_{1-x}\mathrm{Ca}_x\mathrm{MnO}_{3-\delta}$ but shifted to higher values of 2+ doping since Nd is smaller than Ca.[10] The concentration of maximal $T_{\mathrm{MI}}$ corresponds to the concentration at which the posited polaronic phase is least stable relative to the low-temperature metallic phase. Since the lower temperature magnetic phase is stabilized by electronic hopping,[14] whereas a polaronic (or other localized) phase is favored for lower Fermi velocity, we identify the concentration of maximal $T_{\mathrm{MI}}$ with the concentration of maximal bare Fermi velocity.[31] Although a rigid band model is not strictly accurate, the doping dependence of the density of states and bare Fermi velocity should provide a rough guide to the energy dependence of these band parameters above $T_{\mathrm{MI}}$. For doping levels above optimal, the Fermi velocity and density of states increase with increasing energy. For $2+$ concentrations below that of the highest $T_{\mathrm{MI}}$, the Fermi velocity and density of states decrease with increasing energy. For doping levels $x \approx x_c$ with maximal $T_{\mathrm{MI}}$, $N(E)$ and the bare $v_F$ are weak functions of $E$.

We now use this information to deduce the energy dependences of $\sigma_0$ and $E_a$ and thereby account for the qualitative features of the high-temperature thermopower. The term in the thermopower proportional to $d\sigma_0/dE$ is proportional to $dN(0)/dE$. This contribution to $S$ tends to be positive for $x<x_c$ and negative for $x>x_c$ and is weakly temperature dependent. The activation energy $E_a$ is most strongly energy dependent in the temperature range in which the polarons are on the edge of unbinding. At higher temperatures the activation energy is more weakly energy dependent. Well below the transition the magnetization is nearly constant and the activation energy is small ($E_a << kT_{\mathrm{MI}}$). In the intermediate region the activation energy is a sensitive function of the Fermi velocity, with higher Fermi velocity implying smaller activation energy. Therefore, for $x<x_c$ we obtain $dE_a/dE>0$ and this contribution to the thermopower is positive. For $x>x_c$ the hopping barrier decreases with increasing energy, so the contribution to the thermopower from the energy dependence of the hopping barrier is negative.

For doping levels significantly below $x_c$ the hopping barrier term contributes a large positive peak in $S(T)$ near and above $T_{\mathrm{MI}}$, while the density of states term yields a significant, more nearly temperature-independent positive contribution above $T_{\mathrm{MI}}$. This situation is instantiated by sample 1, with a moderate temperature dependence above $T_{\mathrm{MI}}$ due to the energy dependence of both $N(0)$ and $E_a$, and a swift decrease of the thermopower below $T_{\mathrm{MI}}$ due to the abrupt decrease (and strong energy dependence) in $E_a$. The large absolute value of the thermopower is consistent with suboptimal doping.

For doping levels yielding maximum $T_{\mathrm{MI}}$ the density of states and Fermi velocity are weak functions of energy. We expect that the hopping barrier term dominates the thermopower. For $2+$ cation concentrations slightly greater than $x_c$ the thermopower should have a sharp negative peak near $T_{\mathrm{MI}}$, similar to what is observed for sample 2. The small absolute value of the thermopower relative to sample 1 is consistent with the higher value of $T_{\mathrm{MI}}$ in sample 2, since higher $T_{\mathrm{MI}}$ implies closer to optimal doping.[32] The more gradual temperature dependence of the high temperature thermopower for sample 3 may arise from slightly off-optimal doping.

The preceding discussion began with the assumption that the conduction is dominated by carriers near the Fermi energy. Detailed analysis of the temperature dependence of the thermopower above the transition provides information about the conduction process and allows us to test this assumption. In a semiconductor where conduction occurs at energies far from the Fermi level the conductivity varies as $\sim e^{-E_{\mathrm{sc}}/kT}$ and the thermopower varies roughly as $\sim E_{\mathrm{sc}}/kT$, where $E_{\mathrm{sc}}$ is the energy to excite carriers into partially occupied band states. If an attempt to fit to these functional forms for semiconductors yields substantially different values of $E_{\mathrm{sc}}$ from the thermopower and the resistivity in a given material, then the conduction in this family is likely not semiconductorlike and charge transport is more likely dominated by hopping of carriers near the Fermi energy. Sample 1 provides a wide enough temperature range to allow determination of $E_{\mathrm{sc}}$ from both the thermopower and the conductivity. We obtain $E_{\mathrm{thermopower}} \sim 100$ K and $E_{\mathrm{conductivity}} \sim 1000$ K, a clear counterexample to semiconductive behavior and an indication that conduction at high temperatures in these manganite materials procedes via hopping, not semiconduction.

Further analysis sheds more light on the character of the hopping process. The inset of Fig. 1 shows the logarithm of the resistivity for sample 3 plotted against $T^{-1/4}$. The plot is linear from the highest temperature measured, 350 K, down to the resistive transition at $\sim 200$ K, over nearly two decades in resistance. A similar plot for the data at $H=5$ T is linear in a more restricted range above the resistive transition temperature, with fluctuations setting in near $T_{\mathrm{MI}}$. Interestingly, a similar analysis for samples 2 and 3 (not shown) does not yield any simple $\ln\sigma$ versus $T^n$ dependence. Although the standard variable-range-hopping model implies $S \rightarrow 0$ as $T \rightarrow 0$, the previously discussed temperature evolution of the energy dependence of the electronic structure in the manganites reconciles the observed temperature dependence of $S$ in the high-temperature hopping phase with the contrary expectations of the standard variable range hopping model as $T \rightarrow 0$.

An alternative plot (not shown) of $\ln\rho$ versus $T^{-1/2}$ which tests the Efros form for hopping with an exciton-induced pseudogap at the Fermi level[26] yields a sublinear relation between $\ln\rho$ and $T^{-1/2}$, as would be expected for substantial thermal excitation across a hypothetical Coulomb pseudogap. Estimating the crossover temperature $T_E$ below which Efros hopping occurs, $T_E \sim e^4 a N(0)/\epsilon$ with a density of states of $N(0) \sim 2\times10^{-18}\ \mathrm{cm}^{-3}$, [27] a hopping distance of $a \sim 100$ Å (Ref. 27) and a dielectric constant of $\epsilon \sim 10$, we obtain $T_E \sim 5\ \mathrm{K} \ll T_{\mathrm{MI}} \sim 200$ K. In the high-temperature phase the sample is well above any crossover to low-temperature Efros hopping behavior.

Variable-range hopping arises from the competition between the need for hopping sites to be close both in real space and in on-site electronic energy. In three dimensions the optimal hopping distance varies with temperature in such a manner that $\rho \sim e^{aT^{-1/4}}$.[28] Variable-range hopping applies to disordered systems in which conduction proceeds by hopping between randomly located sites with a distribution of allowed electronic energy levels. Both cation disorder[19] and local spin disorder in the high-temperature nonmagnetic phase provide a near-random distribution in electronic on-site energies. The double-exchange lattice polaron model differs from standard variable-range hopping in that the position occupied by a conduction electron is special, lowered by $E_a$ from the random distribution of on-site energies on nearby sites. Taking into account the energetic offset of the localized charge carrier modifies the conduction process and yields a conductivity[33]

$$\sigma \sim \exp\left[-\frac{E_a-\Delta/2}{kT}-\left(\frac{\alpha^3}{k\beta}\right)^{1/4}T^{-1/4}\right]. \tag{3}$$

The energy $\Delta$ is the width of the distribution in on-site energies; $\alpha$ is the inverse linear polaron dimension; $\beta$ is the density of states to within a factor of order unity. $E_a$ is the activation energy to hop from the occupied state to the center of the distribution in on-site energies. If $E_a<\Delta/2$ the conduction reverts to standard variable-range hopping. For reasonable choices of parameters, the two contributions to the exponent are roughly comparable, suggesting that $\ln\sigma \sim T^{1/4}$ behavior may be seen, but in a material-dependent fashion.[34] The qualitative energy dependence as a function of doping for the conductivity in this skewed variable-range-hopping model is broadly similar to that of Eq. (2). Returning to samples 2 and 3, short-range spin order reduces the activation energy $E_a(T)$ as the transition is approached from above. Thus the contribution to the conductivity of the form $e^{-E_a(T)/T}$ does not induce as much upward curvature in $\rho(T)$ as would be expected for a temperature-independent $E_a$. This result is in accord with the experimental resitivity curves for samples 2 and 3, which are not well-fit by Eq. (3) unless $E_a$ is allowed to decrease with decreasing temperature.

One remaining puzzle is the rather large value of the resistivity in the ostensibly metallic region below $T_{\mathrm{MI}}$. At the metal-insulator transition, the carrier hopping barrier drops to values comparable to or below $kT_{\mathrm{MI}}$ itself, so that the carriers are thermally unbound. At lower temperatures, however, a negative temperature coefficient of the resistivity can reappear as the magnetization saturates and the temperature drops below the now temperature-independent carrier activation energy. Such behavior is seen in some underdoped manganite samples.[33] An incipient localization may be consistent with the large absolute value of the resistivity in the metallic low-temperature phase. The supposition of incipient localized behavior at low temperatures provides a possible explanation for the large pressure derivative of the resistivity at low temperatures.[35]

We note that it can be difficult to distinguish between polaronic and Anderson localized phases on the basis of transport data alone, since both yield an activated conduction. For disorder-induced localization it is plausible that the changes in band structure at the transition shift the Fermi level from localized to extended states. The bulk of the preceding discussion on the doping and temperature dependence of the thermopower above $T_{\mathrm{MI}}$ may still apply if the charge localization in the high-temperature phase arose from Anderson localization instead of polaron distortions, since the same qualitative dependences of activation energy upon effective Fermi velocity and density of states could be expected. However, the evolution in the strength of the disorder with increasing cation concentration complicates the doping dependence of $E_a$ in such a model. Experimental probes of the local structural order in the high-temperature phase and across the magnetic transition may help distinguish between these mechanisms.

The resisitivity as a function of temperature in the doped manganites exhibits three regimes: high-temperature activated conduction, an abrupt drop in resistivity associated with magnetic ordering, and low-temperature metalliclike conduction with an unexpectedly large absolute value of the resistivity. The thermopower also has three regimes. Activated conduction yields a high-temperature thermopower of doping-dependent sign and magnitude. Band splitting and formation of a more dispersive partially occupied spin-majority band near the magnetic transition imply an abrupt drop in the thermopower to values more characteristic of metals. The more metallic nature of the electronic structure at lower temperatures yields a more weakly doping-dependent thermopower. Band offsets arising from the $2+/3+$ cation distribution can account for a sign change in the thermopower around 100—150 K. In general, the conduction process in the localized high-temperature phase is more sensitive to variation in the effective bare Fermi velocity than is the low-temperature metallic phase, yielding a stronger doping dependence to the thermopower in the high-temperature regime. The high-temperature charge transport is analyzed within a modified variable-range-hopping model, which suggests that $\sigma \sim e^{aT^{-1/4}}$ may be observed in a restricted range of parameter space.

This work was supported by National Science Foundation Grants No. DMR91-20269 and DMR94-04755 and by the Director, Office of Energy Research, Office of Basic Energy Sciences, Materials Sciences Division of the U.S. Department of Energy under Contract No. DE-AC03-76SF00098. Y.X.J. and A.Z. acknowledge the support of the Miller Institute for Basic Research at the University of California at Berkeley.

---

[1] R. M. Kusters, J. Singleton, D. A. Keen, R. McGreevy, and W. Hayes, Physica B **155**, 362 (1989).

[2] S. S. Manoharan, N. Y. Vasanthacharya, M. S. Hegde, K. M. Satyalakshmi, V. Prasad, and S. V. Subramanyam. J. Appl. Phys. **76**, 3923 (1994).

[3] R. von Helmolt, J. Wecker, B. Holzapfel, L. Schultz, and K. Samwer, Phys. Rev. Lett. **71**, 2331 (1993).

[4] H. L. Ju, C. Kwon, Q. Li, R. L. Green, and T. Venkatesan, Appl. Phys. Lett. **65**, 2108 (1994).

[5] S. Jin, T. H. Tiefel, M. McCormack, R. A. Fastnacht, R. Ramesh, and L. H. Chen, Science **264**, 413 (1994).

[6] K. I. Chahara, T. Ohno, M. Kasai, and Y. Kozono, Appl. Phys. Lett. **63**, 1990 (1993).

[7] R. von Helmolt, L. Haupt, and K. Barner, Solid State Commun. **82**, 693 (1992).

[8] M. McCormack, S. Jin, T. H. Tiefel, R. M. Fleming, J. M. Phillips, and R. Ramesh, Appl. Phys. Lett. **64**, 3045 (1994). A portion of the data missing from Ref. 5 can be found in this work.

[9] H. Y. Hwang, T. T. M. Palstra, S.-W. Cheong, and B. Batlogg, Phys. Rev. B **52**, 15 046 (1995).

[10] H. Y. Hwang, S.-W. Cheong, P. G. Radaelli, M. Marezio, and B. Batlogg, Phys. Rev. Lett. **75**, 914 (1995).

[11] P. Schiffer, A. P. Ramirez, W. Bao, and S.-W. Cheong, Phys. Rev. Lett. **75**, 3336 (1995).

[12] Y. X. Jia, L. Lu, K. Khazeni, D. Yen, C. S. Lee, and A. Zettl, Solid State Commun. **94**, 917 (1995).

[13] Y. X. Jia, L. Lu, K. Khazeni, V. H. Crespi, M. L. Cohen, and A. Zettl, Phys. Rev. B **52**, 9147 (1995).

[14] K. Khazeni, Y. X. Jia, L. Lu, V. H. Crespi, M. L. Cohen, and A. Zettl, Phys. Rev. Lett. **76**, 295 (1996).

[15] T. Kobayashi, H. Takizawa, T. Endo, T. Sato, and M. Shimada, J. Solid State Chem. **92**, 116 (1991).

[16] A series of early work on these materials includes A. H. Morris, B. J. Evans, J. A. Eaton, and L. K. Leung, Can. J. Phys. **47**, 2691 (1969); L. K. Leung, A. H. Morrish, and C. W. Searle, *ibid.* **47**, 2697 (1969); C. W. Searle and S. T. Wang, *ibid.* **47**, 2703 (1969); M. J. Oretzki and P. Gaunt, *ibid.* **48**, 346 (1970); C. W. Searle and S. T. Wang, *ibid.* **48**, 2023 (1970).

[17] D. Elwell and H. J. Scheel, *Crystal Growth from High-Temperature Solutions* (Academic, New York, 1975).

[18] Resistivity decreases with increasing doping level until the antiferromagnetic phase at doping levels above 0.5 is approached. Although sample 1 is doped with Pb, and samples 2 and 3 are doped with a mixture of Pb and Sr, the functional forms of the transport coefficients in the manganites are expected to be insensitive to the particular dopant used. The ionic size of the dopant affects $T_{\rm MI}$, but not the qualitative form of the resistivity at any particular $T_{\rm MI}$ (Ref. 10).

[19] W. E. Pickett and D. J. Singh, Europhys. Lett. **32**, 759 (1995).

[20] In the context of a purely metallic thermopower, the consistent position of the sign change is surprising. Alternatively, a thermally induced shift from band conduction to hopping conduction could induce a similar sign change in the thermopower (Ref. 28) if conduction shifts from primarily electronlike extended states in the majority-spin bands to slightly lower energy ''holelike'' localized states at lower temperatures. A small carrier activation energy in the low-temperature phase could induce incipient localization at low temperatures, perhaps sufficient to cause a sign change in the thermopower. This mechanism must remain speculative until more is known about the density and character of the localized states. The slight upturn in the resistivity at the lowest temperatures in sample 3 lends some support to this explanation.

[21] A. Asamitsu, Y. Moritomo, Y. Tomioka, T. Arima, and Y. Tokura, Nature (London) **373**, 407 (1995).

[22] C. Zener, Phys. Rev. **82**, 403 (1951).

[23] P.-G. DeGennes, Phys. Rev. **118**, 141 (1960).

[24] G. H. Jonker and J. H. Van Santen, Physica XVI, 337 (1950).

[25] A. J. Millis, B. I. Shraiman, and R. Mueller (unpublished).

[26] A. L. Efros and B. I. Shklovskii, J. Phys. C **8**, L49 (1975).

[27] L. Lu, Y. X. Jia, K. Khazeni, and A. Zettl (unpublished).

[28] N. F. Mott and E. A. Davis, *Electronic Processes in Noncrystalline Materials* (Clarendon, Oxford, 1979).

[29] Strictly speaking, the conductivity has a two-component form, with contributions from spin-majority and spin-minority carriers. In a fully spin-disordered high-temperature phase the two contributions would be identical. Far below the transition, the conductivity is dominated by the spin-majority carriers.

[30] We assume that the energy dependences of the hopping distance, hopping attempt frequency, and wave-function overlap terms are either small or follow the same qualitative energy dependence as the hopping barrier.

[31] The reduction in bare effective Fermi velocity above but near $T_{\rm MI}$ at higher doping levels may be due to competition with an incipient antiferromagnetic phase, and not band emptying beyond one half. The term ''bare'' refers to the Fermi velocity before renormalization and consequent localization by the electron-phonon interaction. If one is uncomfortable with the use of Fermi velocity for a double-exchange spin-disordered system, one can alternatively phrase the discussion in terms of average electronic residency time on a given site.

[32] The explanation of the negative peak in the thermopower at high doping is independent of the detailed mechanism for the increased stability of the high-temperature phase at doping levels above that of maximal $T_{\rm MI}$. So long as a decrease in doping corresponds to an increase in polaron activation energy, the sign of the thermopower follows from treating doping dependence as a crude surrogate for energy dependence.

[33] Y. X. Jia, V. H. Crespi, K. Khazeni, L. Lu, A. Zettl, and M. L. Cohen (unpublished).

[34] Alternatively, variable-range hopping may not be operative in some samples because the hopping occurs predominately across the minimal allowed distance for all temperatures above $T_{\rm MI}$.

[35] K. Khazeni, V. H. Crespi, Y. X. Jia, L. Lu, A. Zettl, and M. L. Cohen (unpublished).